Raman Spectrum of Long-Wavelength Phonons in Tetragonal Barium Titanate

L. RIMAI, J. L. PARSONS, AND J. T. HICKMOTT

Scientific Laboratory, Ford Motor Company, Dearborn, Michigan

AND

T. NAKAMURA*

Institute of Solid State Physics, University of Tokyo, Tokyo, Japan

(Received 13 November 1967)

Polarized Raman spectra of tetragonal $BaTiO_3$ have been obtained at room temperature with He–Ne laser excitation. Using several different crystallographic directions for the phonon wave vector $\mathbf{q}$, most of the vibrational modes for $\mathbf{q}\sim 0$ have been classified using Raman data alone. Three pairs of longitudinal-transverse A_1 modes have been observed with frequencies which semiquantitatively satisfy the Lyddane-Sachs-Teller relationship. A low-frequency transverse E mode has been observed at 10 cm^{-1} and assigned to the ferroelectric soft-mode system. The soft-mode result has been discussed in terms of the effect of damping on the dispersion relation. These results are not in good agreement with those derived previously by multiparameter fits to the infrared reflectivity data.

1. THEORETICAL INTRODUCTION

At room temperature, the space group of $BaTiO_3$ is[1,2] C_{4v}^1 ($P4mm$). However, the long-wavelength vibrations active in the intrinsic first-order Raman spectrum can be classified according to their transformation properties under the operations of the factor group isomorphous with the C_{4v} point group. In addition to crystal-field considerations, the frequencies of the various infrared (IR) active modes will be affected by the associated electric field[3,4]; because of the absence of inversion in C_{4v} symmetry, such will be the case for most all Raman active modes. For some highly symmetric crystallographic directions of the phonon wave vector $\mathbf{q}$, one can predict, in a simple manner, the types of vibrational modes that will be present. One can indeed find a number of simple experimental configurations that yield spectra with sufficient information that most vibrational modes of wave vector $\mathbf{q}\sim 0$ can be classified using Raman data alone. It is the aim of this paper to describe just such an investigation, and then discuss its results in the face of those obtained from other measurements.[5–9] Part of such results on Raman spectra have been summarized previously (Pinczuk *et al.*[10] and Parsons and Rimai[11]); these are appreciably extended here, and the basis for interpretation is much more fully discussed.

In the cubic phase of $BaTiO_3$, all vibrations are triply degenerate: three infrared-active T_2 modes and one T_1 mode inactive in infrared absorption.[12] In the tetragonal phase, the degeneracy of each of these modes is split by the action of the lowered crystal-field symmetry, and for the T_2 phonons by the additional electromagnetic interaction involving the electric polarization associated with the vibration.[9] For the case of tetragonal symmetry, the differential equations governing the propagation of these phonons, for sufficiently long wavelength (such that phase difference between neighboring cells can be neglected), may be stated as follows (assuming waves of form $\exp[i(\mathbf{q}\cdot\mathbf{r}-\omega t)]$ with no damping, i.e., both $\mathbf{q}$ and ω real):

$$-\omega^2\mathbf{W}=\mathbf{b}_{11}\cdot\mathbf{W}+\mathbf{b}_{12}\cdot\mathbf{E}, \tag{1}$$

$$\{(\omega^2/c^2)(\mathbf{1}+4\pi\mathbf{b}_{22})\cdot\mathbf{q}^2\}\mathbf{E}=-\mathbf{q}(\mathbf{q}\cdot\mathbf{E})-(\omega^2/c^2)4\pi\mathbf{b}_{21}\cdot\mathbf{W}, \tag{2}$$

$$\mathbf{q}\cdot\mathbf{E}=4\pi\mathbf{q}\cdot[\mathbf{b}_{21}\cdot\mathbf{W}+\mathbf{b}_{22}\cdot\mathbf{E}]. \tag{3}$$

With the mechanical-electrical coupling tensors $\mathbf{b}_{12}=\mathbf{b}_{21}=0$, Eq. (1) reduces to the equation for a harmonic mechanical oscillation $\mathbf{W}$, Eq. (2) to the wave equation for an electric vector $\mathbf{E}$, and Eq. (3) corresponds to $\nabla\cdot\mathbf{D}=0$. The quantity $\mathbf{1}+4\pi\mathbf{b}_{22}=\boldsymbol{\varepsilon}(\infty)$ would correspond to the optical dielectric tensor had we a simple crystal with only this one vibrational mode (other than the sound waves). This theory was developed under the

* Work performed at Ford Scientific Laboratory while on leave from University of Tokyo.

[1] F. Jona and G. Shirane, *Ferroelectric Crystals* (Pergamon Press, Inc., New York, 1962).

[2] W. Känzig, *Ferroelectrics and Antiferroelectrics in Solid State Physics* (Academic Press Inc., New York, 1957), Vol. IV, p. 165.

[3] M. Born and K. Huang, *Dynamical Theory of Crystal Lattices* (Clarendon Press, Oxford, England, 1954).

[4] R. Loudon, Advan. Phys. **13**, 423 (1964).

[5] W. G. Spitzer, R. C. Miller, D. A. Kleinman, and L. E. Howarth, Phys. Rev. **126**, 1710 (1962).

[6] A. S. Barker and M. Tinkham, Phys. Rev. **125**, 1527 (1962).

[7] A. S. Barker and J. J. Hopfield, Phys. Rev. **135**, A1732 (1964).

[8] J. Ballantyne, Phys. Rev. **136**, A429 (1964).

[9] S. Ikegami, J. Phys. Soc. Japan **19**, 46 (1964).

[10] A. Pinczuk, W. Taylor, E. Burstein, and I. Lefkowitz, Solid State Commun. **5**, 429 (1967).

[11] J. L. Parsons and L. Rimai, Solid State Commun. **5**, 425 (1967).

[12] R. A. Cowley, Phys. Rev. **134**, A981 (1964).

fundamental assumption that the dielectric response of the lattice is independent of the spatial distribution of the field **E**, i.e., the tensors **b** have no explicit dependence on **q**. Actually, because of the finite wavelength of the excitations involved in the experiments, $\mathbf{b}_{11}$ may depend slightly on **q**, especially on its direction, as one indeed finds in the experimental results.

For a tetragonal symmetry, we choose axes $\hat{x}\hat{y}\hat{z}$, with $\hat{z}$ the $\hat{c}$ axis and $\hat{x}$, $\hat{y}$ the $\hat{a}$ axes. The second-rank tensors will be diagonal, with $b^{zz}=b^c$, b^{xx}, $b^{yy}=b^a$. We now take the solutions of the eigenvalue problem implied by Eqs. (1) and (2) [only five independent components due to condition (3)] for a few particularly simple cases of interest.

(1) $\mathbf{q}=q\hat{x}$. We have one longitudinal

$$\mathbf{W}=W_x\hat{x}, \qquad \mathbf{E}=E_x\hat{x},$$

$$E_x=-[4\pi b_{21}{}^a/(1+4\pi b_{22}{}^a)]W_x,$$

with frequency

$$\omega_{la}{}^2=-b_{11}{}^a+[4\pi b_{12}{}^a b_{21}{}^a/(1+4\pi b_{22}{}^a)]=-b_{11}{}^a+\omega_{pa}{}^2,$$

and two pairs of transverse modes with electric fields and frequencies depending on **q** in such a way that for large **q** there is one pair that has zero macroscopic electric field. The other pair corresponds to a purely electromagnetic wave and is of no further interest (for the **q** values involved in 90° Raman scattering). In this limit for the transverse phonon branch (the mechanical mode), one obtains for $W=W\hat{y}$,

$$\omega_{ta}{}^2=-b_{11}{}^a,$$

for $W=Wz$,

$$\omega_{tc}{}^2=-b_{11}{}^c.$$

(2) $\mathbf{q}=(q/\sqrt{2})(\hat{x}+\hat{y})$. For this case, we have the same frequencies:

$$\mathbf{W}=W\hat{z}\Rightarrow\omega_{tc}{}^2=-b_{11}{}^c,$$

$$\mathbf{W}=(W/\sqrt{2})(\hat{x}+\hat{y})\Rightarrow\omega_{la}{}^2=\omega_{ta}{}^2+\omega_{pa}{}^2,$$

$$\mathbf{W}=(W/\sqrt{2})(\hat{x}-\hat{y})\Rightarrow\omega_{ta}{}^2=-b_{11}{}^a.$$

The difference between cases (1) and (2) is important as far as the selection rules are involved.

(3) $\mathbf{q}=q\hat{z}$. We have longitudinal mode

$$\mathbf{W}=W\hat{z}\Rightarrow\omega_{lc}{}^2=\omega_{tc}{}^2+\omega_{pc}{}^2=-b_{11}{}^c+[4\pi b_{21}{}^c/(1+4\pi b_{22}{}^c)],$$

and transverse modes

$$\mathbf{W}=W\hat{x} \quad \text{or} \quad \mathbf{W}=W\hat{y}\Rightarrow\omega_{ta}{}^2=-b_{11}{}^a.$$

(4) $\mathbf{q}=(q/\sqrt{2})(\hat{z}+\hat{x})$. We have transverse mode

$$\mathbf{W}=W\hat{y}\Rightarrow\omega_{ta}{}^2=-b_{11}{}^a$$

and a pair of mixed modes. For these, still in the limit of large **q**, one can derive the following simple equations:

$$W_x(\omega^2-\omega_{la}{}^2)-W_z\omega_p{}^2=0,$$

$$-W_x\omega_p{}^2+W_z(\omega^2-\omega_{lc}{}^2)=0,$$

with

$$\omega_p{}^2=[4\pi/(1+4\pi b_{22})]b_{12}{}^a b_{21}{}^c \qquad (4)$$

[with the additional assumption of an isotropic $\mathbf{b}_{22}$, which is reasonable in view of the relatively small anisotropy in $\boldsymbol{\varepsilon}(\infty)$]. Then, the frequencies of the mixed modes are given by

$$\omega^2=\tfrac{1}{2}(\omega_{la}{}^2+\omega_{lc}{}^2)\pm\tfrac{1}{2}[(\omega_{la}{}^2-\omega_{lc}{}^2)^2+4\omega_p{}^2]^{1/2}, \qquad (5)$$

which, in combination with Eq. (4), gives the ratio of W_z to W_x present in each of the modes (or the ratio of A to E or B_1 to E components).

Given the directions of incident and scattered electric vectors $\mathbf{E}_\mu$ and $\mathbf{E}_\nu$, the Raman cross section for a scattering by a given mode is proportional to the square of the corresponding component of a second-rank tensor $\alpha_{\mu\nu}$.[4] The nonzero components of this tensor for a mode with a given symmetry-displacement direction, i.e., displacement transforming according to a given irreducible representation, can be derived from the knowledge of the C_{4v} point group; the mixed modes above have a superposition of such displacements, and the corresponding Raman tensor will also be a superposition. For our choice of coordinates, for $\mathbf{W}=W\hat{z}$ (A_1 or B_1 mode), $\alpha_{\mu\nu}=\delta_{\mu\nu}\alpha_\mu$; for $\mathbf{W}=W\hat{x}$, $\alpha_{\mu\nu}=0$, except $\alpha_{zy}=\alpha_{yz}$ (E_1 mode).

The preceding considerations were made neglecting any damping mechanism, either mechanical (due, in general, to anharmonicity) or electrical (conductivity effects). However, the necessity of assuming large damping for some of the modes has been concluded from the study of the IR reflectivity of materials such as $BaTiO_3$.[5,6]

In a later section, we discuss how such effects relate to the Raman measurements; we present here the pertinent basic points.

Because of the importance of momentum conservation in defining the Raman selection rules, it is most convenient to describe damped excitations by a wave of real momentum $\hbar\mathbf{q}$, but complex frequency $\omega=\omega'+i\omega$. We can add a mechanical damping term to the left of Eq.(1) as $-i\gamma\omega\mathbf{W}$. A finite conductivity σ adds a term $(4\pi\sigma\omega i/c^2)\cdot\mathbf{E}$ to the left side of Eq. (2). For a case where we have pure transverse and longitudinal modes, say, $\mathbf{q}=q\hat{x}$, the complex longitudinal frequency will be the solution, with appropriate sign of ω', of

$$\omega^2+i\gamma^a\omega-\omega_{la}{}^2=0. \qquad (6)$$

The equation for the transverse frequencies is

$$c^2q^2/\omega^2=1+4\pi b_{22}{}^{a,c}-[4\pi b_{21}{}^{a,c}b_{12}{}^{a,c}/(\omega^2-\omega_{ta,c}{}^2+\gamma^{a,c}\omega i)]$$
$$+4\pi(1+4\pi b_{22}{}^{a,c})(\sigma^{a,c}/\omega)i. \qquad (7)$$

We see from Eq. (6) that the half-width of the longitudinal mode will be determined in a simple manner by γ. If $\gamma \ll \omega_l$, this half-width will give γ^a directly. As the damping increases, it will begin to contribute also to the real part of ω; for the mode where damping is most important, such an effect should be more marked for the transverse vibrations, since $\omega_{ta} \ll \omega_{la}$. As we shall see later, at least according to this simple picture, the Raman results are inconsistent with the large damping invoked in some of the analyses of IR reflectivity data.[5–7] In a material such as $BaTiO_3$, because of the large ratio $\varepsilon(0)/\varepsilon(\infty)$, one expects at least one IR active mode system (i.e., group of three modes originating from one T_2 mode of the cubic phase) with a large ratio ω_l^2/ω_t^2; in particular, the simplest model for this material predicts one rather low-lying transverse E mode (ω_{la}); one should expect also for the corresponding A mode, $\omega_{lc} > \omega_{tc}$, but with a much smaller ratio than for the associated E modes.[13–15] The presence of such a "soft" mode has been substantiated earlier by inelastic neutron scattering in strong paraelectric materials such as $SrTiO_3$ [12] and $KTaO_3$,[16] as well as most recently in the paraelectric phase of $BaTiO_3$.[17] It has also been observed in the Raman spectra of $SrTiO_3$ [18–20] and $KTaO_3$, and its presence indicated by analysis of IR reflectivity data. Pinczuk *et al.*[10] and, more recently, DeDomenico *et al.*,[21] in their study of the Raman spectrum of $BaTiO_3$, have reported the presence of a low-frequency tail corresponding to inelastic scattering by a vibration of E character. In Sec. III, we report our results on this mode at room temperature, wherein a reasonably well resolved line appears superposed to the low-frequency tail. In Sec. II, we present a short discussion of some of the experimental aspects of this work. In Sec. III, we present the data which are discussed in Sec. IV in accordance with the general considerations presented above.

2. REMARKS ON EXPERIMENTAL TECHNIQUES

The exciting radiation was obtained from a Spectra Physics 125 He–Ne laser, at 6328 Å. Measurements in all but the low-frequency region, corresponding to the softest mode, were made with a conventional synchronous detector. The scattered radiation was analyzed, using a converted Perkin-Elmer model 99G double-pass monochromator, using slit width corresponding to spectral resolution of about 5 cm^{-1}. A cold-N_2-gas-cooled 7265 photomultiplier (P.M.) was used as a detector.

The technique used to record the low-frequency region deserves some further discussion. For Raman shifts under, say, 15 cm^{-1}, at least for the quality of $BaTiO_3$ crystals available to us, one encounters a severe dynamic-range problem due to the presence of the low-frequency tails; actually, as some evidence indicates, part of this tail could be also due to scattering from sound waves, which, usually, has a cross section about two orders of magnitude larger than that from optic-type vibrations. Dynamic-range limitations are overcome by using, in lieu of high-gain amplification, data accumulation in digital form.

To record the low-frequency spectra, the slits of the monochromator were closed to 5 μ, yielding a spectral resolution better than 0.75 cm^{-1}. They were also appropriately masked to minimize the amount of first-pass radiation reaching the exit slit, in order to reduce its contribution to the photon-shot noise. The output of the P.M. was processed in a digital up-down counting system[22] consisting of an amplifier, pulse-height discriminator, and digital memory of a 1024-channel analyzer for accumulation. The analyzer input was run in the add-subtract mode, in synchronization with the chopper acting on the second-pass radiation only. This synchronization was supplied by the 13-cps chopper of the model 99G. Signal and background pulses were added and background pulses subtracted for precisely equal times. This results in a $\sqrt{2}$ decrease in signal-to-noise ratio, which was not considered harmful in this case. The channel advance was supplied by a binary count-down from the add-subtract control waveform, locking the wavelength drive to the analyzer channel number. Repetitive passes were made to improve the signal-to-noise ratio with weak signals and supply-time averaging.[23] For purposes of comparison, the total accumulation time per channel (number of scans$\times$ scan time/1024) was so adjusted as to yield approximately the same peak value at zero frequency shift (6328 Å) for the light scattered from the sample for the polarization configurations giving the largest elastic peak and for light scattered elastically from a metal plate. For the same accumulation time in different polarization relationships, the variation of this peak for scattering from $BaTiO_3$ certainly was less than an order of magnitude.

A number of different samples from different sources was investigated. Where permitted by sample geometry, experiments with the same configuration of wave vectors

[13] P. W. Anderson, *Fizika Dielektrikov* (Academy of Sciences, USSR, 1960), p. 290.
[14] W. Cochran, Advan. Phys. **10**, 401 (1961).
[15] B. D. Silvermann, Phys. Rev. **135**, A1596 (1964).
[16] G. Shirane, R. Nathans, and V. J. Minkiewicz, Phys. Rev. **162**, 528 (1967).
[17] G. Shirane, B. C. Frazer, V. J. Minkiewicz, J. A. Leake, and A. Linz, Phys. Rev. Letters **19**, 234 (1967).
[18] L. Rimai and J. L. Parsons, Solid State Commun. **5**, 381 (1967).
[19] P. A. Fleury and J. M. Warlock, Phys. Rev. Letters **18**, 665 (1967).
[20] M. J. Weber, R. Schaufele, and B. D. Silverman, Phys. Letters **25A**, 47 (1967).
[21] M. DiDomenico, S. P. S. Porto, and S. H. Wemple, Phys. Rev. Letters **19**, 855 (1967).
[22] F. T. Arrechi *et al.*, Rev. Sci. Instr. **36**, 1685 (1965).
[23] R. A. Ernst, Rev Sci. Instr. **36**, 1685 (1965).

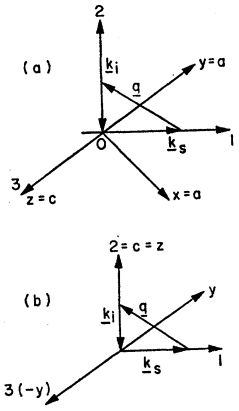

FIG. 1. Raman-scattering configurations.

and electric fields were repeated on all of them. The investigation of the low-frequency spectrum was hindered in the less perfect crystals by the tails of the strong elastic scattering from structure defects. However, its presence was evidence in all samples. For poled samples, we found good agreement on all the results at room temperature, and thus it is reasonable to assume that the room-temperature spectra are essentially intrinsic in nature. The samples used were as follows.

(a) Butterfly plates grown in this laboratory from flux[24] which were usually poled with the $\hat{c}$ axis perpendicular to the large face; for experiments on these, all combinations of propagation directions along the crystal axes were used.

(b) A cylindrical sample grown from the melt[25] which was poled with $\hat{c}$ axis parallel to the cylinder generator, and for which experiments were done with incident momentum in the $\hat{c}$ direction. This was the crystal that gave the best low-frequency spectrum.

(c) A large crystal grown from the flux for which various cuts were made to repeat the experiments in the configurations used with the previous samples and also to enable one to study the phonon propagating along one of the crystallographic axes, as described in the next section.[26]

3. EXPERIMENTAL RESULTS

Because of anisotropy in the optical dielectric constant, one must take care in selecting experimental configurations in which there are no depolarization effects. This essentially requires both the wave vectors of incident and scattered light $\mathbf{k}_i$ and $\mathbf{k}_s$, respectively, to be normal to the surfaces, and also that the corresponding electric vectors $\mathbf{E}_i$ and $\mathbf{E}_s$ be either parallel or perpendicular to the $\hat{c}$ axis. This has been satisfied in all configurations used to deduce data on poled crystals, and is also satisfied for the one particular measurement on an unpoled crystal which is significant for this investigation.

Let us call $\mathbf{q}$ the wave vector of the phonon, and consider first the case (a) $\mathbf{q} \parallel x$ of Fig. 1. 1, 2, and 3 are the axes of reference for the Raman tensor $\alpha_{\mu\nu}$; we then have the following nonzero components:

$$E_{\text{long}} \Rightarrow \alpha_{13} = \alpha_{31} = \tfrac{1}{2}\sqrt{2}\alpha_E,$$

$$E_{\text{trans}} \Rightarrow \alpha_{13} = -\alpha_{31} = \tfrac{1}{2}\sqrt{2}\alpha_E,$$

$$A_{\text{trans}} \Rightarrow \alpha_{33} = \alpha_c,\ \alpha_{12} = \alpha_a,$$

$$B_{\text{trans}} \Rightarrow \alpha_{12} = \alpha_a,$$

and thus we cannot distinguish E_{long} from E_{trans} modes. However, both A_{long} and B_{long} will be rigorously absent.

If we now consider the same configuration, but with the crystal randomly unpoled, and restrict ourselves to the measurement of α_{33}, the condition for no depolarization will be still valid. The following will be the nonzero components:

$$A_{1\ \text{long}},\ \alpha_{33} = \alpha_a,$$

$$B_{1\ \text{long}},\ \alpha_{33} = \alpha_a,$$

$$A_{1\ \text{trans}},\ \alpha_{33} = (\alpha_c^2 + 2\alpha_a^2)^{1/2},$$

$$B_{1\ \text{trans}},\ \alpha_{33} = (2\alpha_a)^{1/2}.$$

Thus, by comparing α_{33} measurements in these two cases, we can identify the longitudinal modes with c-direction mechanical displacements. Since there is no evidence for the presence of a B_1 transverse mode, we shall assume that the three longitudinal modes thus identified are the $A_{1\ \text{long}}$ modes derived from the three IR-active T_2 modes of the cubic phase.

TABLE I. Symmetry species and frequencies for various directions of propagation of the Raman active long-wavelength modes in the tetragonal $BaTiO_3$ lattice.

		Frequencies (cm^{-1})					
T modes (cubic phase)	q	LA_1	TA_1	LE	E	TE	Mixed A_1 and E
ν_1	$\hat{z}$	730					
	$\hat{x}$		528				
	$\hat{x}+\hat{y}$		512		510		
	$\hat{x}+\hat{z}$					505	510
ν_2	$\hat{z}$	465					
	$\hat{x}$		280	(485)			
	$\hat{x}+\hat{y}$		270				
	$\hat{x}+\hat{z}$		270			10	485
ν_3	$\hat{z}$	190					
	$\hat{x}$		170		180		
	$\hat{x}+\hat{y}$		165		172		
	$\hat{x}+\hat{z}$					174	174
ν_4					304		

[24] Graciously supplied by Dr. H. Stadler of this laboratory.
[25] Graciously supplied by Professor F. Brown of Williams College.
[26] Obtained from Professor A. Linz, Crystal Physics Laboratory, MIT.

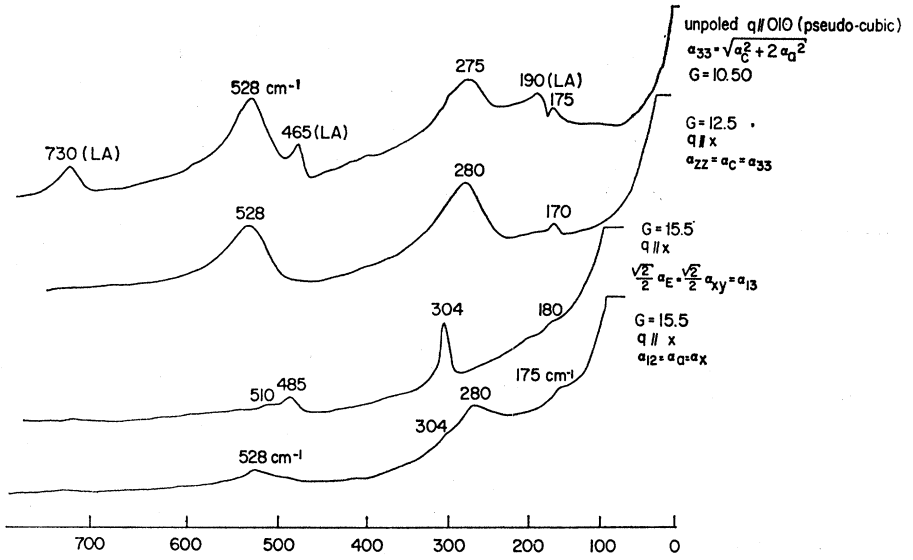

FIG. 2. Raman spectra of tetragonal $BaTiO_3$ for various directions of propagation of q and polarization of $\mathbf{k}_i$ and $\mathbf{k}_s$; $\Delta c=2$ in the amplifier gain setting G is approximately equivalent to a factor of 2 change in signal strength.

The situation for the phonon $\mathbf{q}=\frac{1}{2}\sqrt{2}(\hat{x}+\hat{y})$ is rather similar to the above [case (a)], but with transverse A and E modes present ($\hat{1}=\hat{x}$, $\hat{2}=\hat{y}$, and $\hat{3}=\hat{c}$).

Some useful information can, however, still be gained from the study of the phonon with $\mathbf{q}=\frac{1}{2}\sqrt{2}(\hat{x}+\hat{z})$, Fig. 1(b).

We set $3=-y$, $1=x$, and $2=c=z$, and the nonzero tensor components should be as follows: mixed mode $(A+E)$, α_{33} and α_{32}; E_{trans}, α_{12}. For modes with no electric field, of course, we shall have $A_1 \Rightarrow \alpha_{33}$; $E_x \Rightarrow \alpha_{32}$; $E_y \Rightarrow \alpha_{12}$; and, of course, E_x and E_y being degenerate, $\alpha_{32}=\alpha_{12}$.

We see, then, that with this configuration, it is possible to isolate a transverse E mode with displacement along an **a** axis, which is the softest direction in the crystal [corresponding to the largest $\varepsilon(\sigma)$]. In this direction of propagation, the transverse modes should have purely E character.

There seems to be a broad line centered around 265 cm^{-1} that does not conform to the exclusion conditions required by the selection rules, indicating perhaps that its presence is due to some type of imperfections in the crystal. The frequency of this peak seemed to change somewhat from one crystal to another. It was also found that in both the butterfly and the flux-grown material, the 512 line persisted in forbidden configurations with relatively large intensity, although definitely less than in the permitted configuration according to the assignments discussed later. This seems to go along with the fact that these two lines remain about the tetragonal-to-cubic transition, at least in some of the crystals.[11] On Figs. 2 and 3, we present some of the high-frequency lines.

Figure 4 shows the low-frequency spectrum in the indicated configurations; the stokes and antistokes lines are clearly resolved. The symmetry assignments deduced from the measurements are shown in Table I. We should note, in all fairness, that the LE assignment for the mode at about 485 cm^{-1} is rather uncertain—it is based mainly on its mixed character in a few situations, rather than on a clear-cut determination similar to that for the LA modes. It should also be noted that the assignment of the LA_1 mode at 465 cm^{-1} to the ν_1 system would require large anisotropy in $\nu=\nu(\mathbf{q})$ even at the relatively small **q** involved in Raman scattering for the TA_1 mode at 528 cm^{-1}. Evidence for the latter possibility is provided by the persistence of this line for $T>T_c$, but the existence of such large anisotropy in $\nu=\nu(\mathbf{q})$ for a stable mode is highly improbable.

It has been pointed out[9] that the dielectric properties of perovskite crystals arise from the behavior of the ν_2 mode system. The A_1 component of the system is probably stable and contributes to the relatively normal ϵ_c, while the E component is the low-frequency, unstable ferroelectric mode. Whereas the A_1 modes at 528 and 170 cm^{-1} have associated E modes at 505 and 174 cm^{-1}, respectively, no E mode was found near the A_1 mode at 280 cm^{-1}. The latter has therefore been assigned to the stable part of the soft-mode system, with its associated E mode$\sim$14 cm^{-1}.

4. DISCUSSION

(1) Effect of damping on dispersion relations for IR-active modes. Since, for the soft mode, one finds experimentally a linewidth not negligible compared to its frequency, the effect of damping on the dispersion relations has to be considered in some detail. The equation for the eigenfrequency of the TE modes was given in (7); we shall neglect the effect of finite conductivity. Were this the only IR-active E mode of the

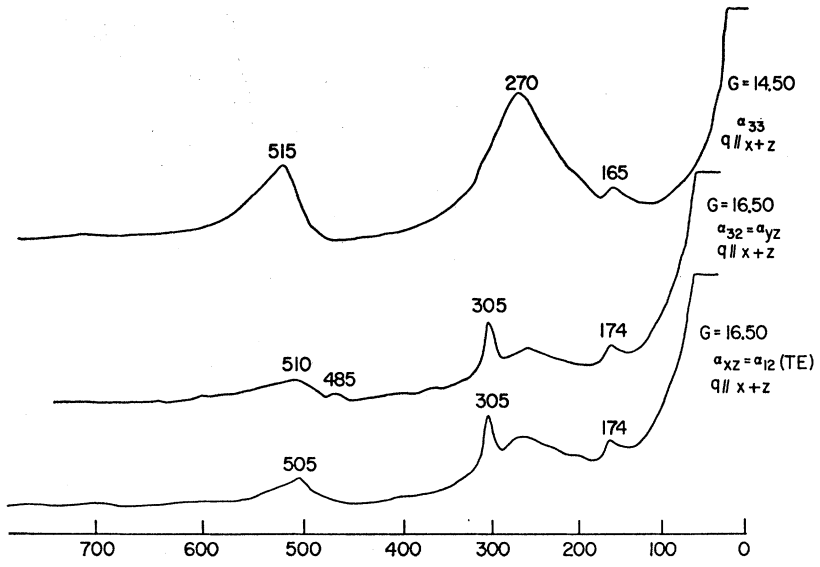

FIG. 3. Raman spectra of tetragonal $BaTiO_3$ for various directions of propagation of q and polarization of $\mathbf{k}_i$ and $\mathbf{k}_s$; $\Delta c=2$ in the amplifier gain setting G is approximately equivalent to a factor of 2 change in signal strength.

crystal, we could make the following identifications:

$$\epsilon_a^{(\infty)}=1+4\pi b_{22}{}^a,$$
$$\epsilon_a^{(0)}-\epsilon_a^{(\infty)}=4\pi b_{21}{}^a b_{12}{}^a, \tag{8}$$

where the ϵ are the a direction dielectric constants in the indicated frequency limits. They are directly related to the coupling parameters between displacement, polarization, and electric field of the excitation. The solutions of (7) give, in general, complex frequencies; the real part locates the corresponding line center in the spectrum, and the imaginary part is a measure of the damping (half-width at half-amplitude). One of the solutions of Eq. (7) has $[\mathrm{Re}(\omega^2)]\sim c^2q^2/\epsilon_a{}^{\mathrm{eff}}(\infty)$, which corresponds to an excitation propagating through the crystal with the speed of light $c/\sqrt{\epsilon}$. It is the electromagnetic branch: The phononlike branch, in the region of wave vectors corresponding to 90° Raman scattering for excitation at 6328 Å$\Rightarrow q\sim 15\,600$ cm^{-1} will have $\omega^2\ll c^2q^2$. We can approximately solve for it by neglecting $\epsilon_a(\infty)$ in (7). Such an approximation should be quite acceptable for a truly soft mode. One obtains

$$\omega_{t0}{}^a=-\tfrac{1}{2}iR\gamma^a+\tfrac{1}{2}(4R\omega_0{}^2-R^2\gamma^2)^{1/2},$$

with

$$R=[1+(\omega_0{}^2\delta/c^2k^2)]^{-1}=[1+\delta(\omega_0/\omega_r)^2]^{-1},$$

where $\delta=\epsilon(0)-\epsilon(\infty)$, and $w_r=cq$ will be in the order of the frequency of incident radiation at $\sim$6328 Å. For any reasonable assumption of parameters, $R\sim 1$, and thus

$$\omega=\tfrac{1}{2}(4\omega_0{}^2-\gamma^2)^{1/2}-\tfrac{1}{2}i\gamma,$$

and for $\omega_0{}^2>\frac{1}{4}\gamma^2$ or $\omega_0>\frac{1}{2}\gamma$, one obtains an actual well-defined line at a finite frequency, depressed, however, from its undamped value ω_0. Actual numerical solutions of the Eq. (7) are shown in Fig. 5; the soft-mode parameters were obtained, assuming it to be solely responsible for $\epsilon_a(0)-\epsilon(\infty)$, with $\omega_L=730$ cm^{-1} as assumed by Barker in the analysis of reflectivity data; thus $\omega_0=33$ cm^{-1}. The damping was varied from Barker's value of 90 cm^{-1} to zero. These results do reveal that even if damping is assumed to be independent of frequency, one may obtain at the larger momenta a well-defined line. This is so in spite of the fact that strong overdamping may have to be assumed to explain spectra such as IR reflectivity which involves excitations of much longer wavelength. However, these calculations also show that quantitative incompatibility between the present Raman results and the soft-mode frequencies and damping derived from the reflectivity fits still remains. If we assume that the relatively narrow peak of E character in Fig. 4 locates the ω' of the soft mode, we obtain[27]

$$\omega'=10\pm 1.5\ \mathrm{cm}^{-1},$$
$$\omega''=\ 4\pm 1.5\ \mathrm{cm}^{-1},$$

which would give the following approximate values

[27] The results of Ref. 21 do not show the presence of the low-frequency peak which, in this work, is assigned to the soft mode. We should note in this connection that as we decrease the instrumental resolution, the strength of the signal from the tail will increase rather rapidly with respect to that of any narrow component. The observation of the latter will then require progressively larger dyanmic range from the detecting apparatus. Our results do not exclude the possibility that the intensity in the broad tail has appreciable contribution from the soft-mode system. This situation would give a different value for the undamped frequency ω_0. However, since the half-power point of this tail is still under 20 cm^{-1} (Ref. 21), it seems unlikely that either ω_0 or γ could be much larger than 20 cm^{-1}.

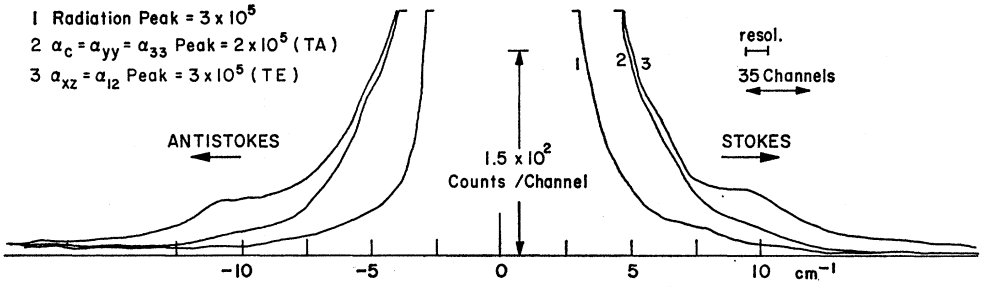

FIG. 4. Low-frequency Raman spectrum of tetragonal $BaTiO_3$.

for the undamped frequency and damping constant:

$$\omega_0 = \sim 12 \pm 2 \text{ cm}^{-1},$$

$$\gamma = 8 \pm 3 \text{ cm}^{-1}.$$

These results are rather close to the values yielded for the lowest-frequency peak of $\epsilon''(\omega)$ as calculated by a direct Kramers-Kronig analysis of the reflectivity data.[8]

The dispersion curves for the above parameters are also plotted in Fig. 5. There are rather interesting implications of the theoretical results presented in Fig. 5. The angular dependence of Raman spectra of strongly damped vibrations could be quite revealing, even at relatively large angles; the damping constant can be obtained from the angular dependence of the peak frequency. Even if a vibration is overdamped, it will give a relatively narrow line at the smaller angles (corresponding to small momentum transfer).

(2) Next, one should consider the applicability of the generalized Lyddane-Sachs-Teller (LST) relations,[19] since we seem to have isolated the three pairs of A_1 modes both longitudinal and transverse. In the cubic phase, we have only three T_2 modes active in the IR. The A_1 modes of the tetragonal phase originate in the removal of the threefold degeneracy of these T_2 modes. It is not entirely unreasonable that, if the general assumptions underlying its derivation (macroscopic local field uniformly determined by polarization and negligible anisotropy because of direct dependence of frequency on momentum, i.e., negligible phase shift between neighboring unit cells) are not too far from

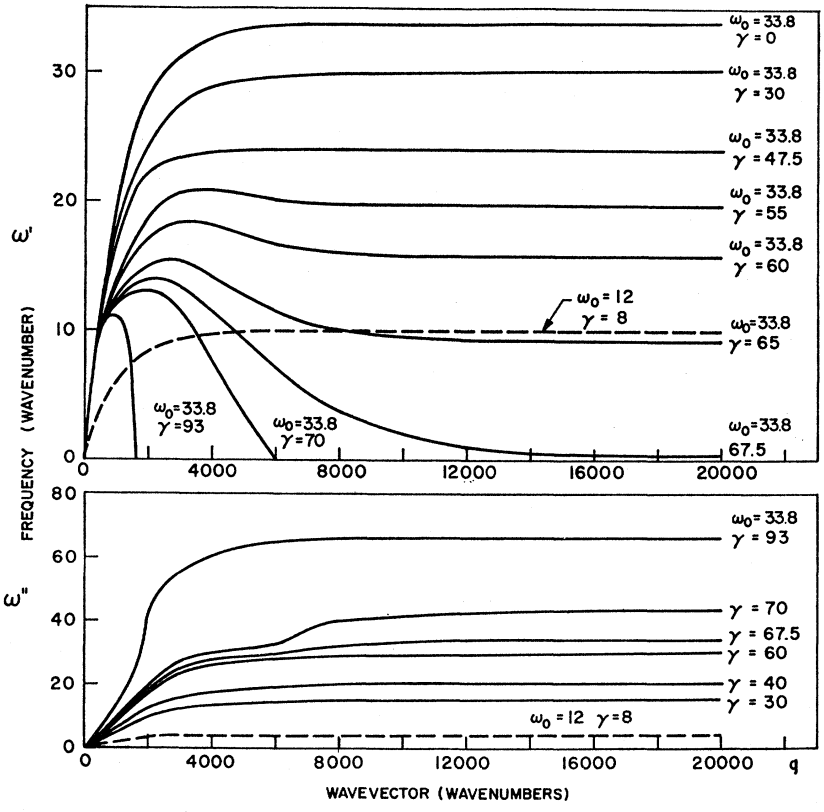

FIG. 5. Real (ω') and imaginary (ω'') parts of solutions of the long-wavelength phonon dispersion relation for various parameter combinations.

the truth, the following relation should hold:

$$\prod_i [\omega_i^L(A_1)]/\prod_i [\omega_i^T(A_1)] = [\epsilon_c(0)/\epsilon_c(\infty)]^{1/2}.$$

From the products of the frequencies one obtains the ratio

$$(190\times 465\times 730/170\times 280\times 528) = 2.57,$$

which should be compared with

$$[\epsilon_c(c)/\epsilon_c(\infty)]^{1/2} \simeq 4\pm 1.$$

The large error limit is due to the large uncertainties in the measurement of $\epsilon_c(0)$.[28,29,1]

In this theory, it is not clear how to account for the B_1 mode for which displacement direction is the same as for A_1 modes; however, neither the parent T_1 mode in the cubic phase nor the B_1 mode is active in the infrared; and the corresponding contributions to the above relation are probably negligible. The discrepancy is probably due to lack of accurate satisfaction of the conditions for the validity of the LST relation. In particular, the presence of non-negligible anharmonic terms in this crystal because of the proximity of the phase transition may cause important deviations.

For the softer direction of the dielectric constant, one has to invoke the E modes, as follows:

$$\prod_i \omega_i^L(E)/\prod_i \omega_i^T(E) = [\epsilon_a(0)/\epsilon_a(\infty)]^{1/2}.$$

Here we know for sure only about two purely TE modes—the soft mode and the mode at $\sim$175 cm^{-1}. Also, in order to apply the above relationships, one probably should use the undamped frequencies, which would then give a rather large uncertainty to the soft-mode frequency, because of the large error in obtaining the linewidth from the experimental data. If one assumes again here, as for the A_1 modes, that the largest contribution to this ratio comes from one single pair of modes, one can try to predict the position of the L-E_1 component of the soft-mode branch: Since $[\epsilon(0)/\epsilon(\infty)]^{1/2} \sim 25$, with $\omega_T(E_1) = 12$ cm^{-1}, one obtains $\omega_L(E_1) \simeq 300$ cm^{-1}; the most reasonable candidate for this is the mode at 485 cm^{-1}, since the mode at 307, as indicated by its negligible angular dependence, must correspond to small IR activity.

These results are not in good agreement with those derived from the reflectivity data.[5–7] One should, however, bear in mind that vibrational frequencies are obtained there as a result of a multiparameter fit; this is so even if the anisotropy of the crystal is not taken into account. Consideration of damping effects in determining the dispersion relations may to some extent decrease this discrepancy: The Raman measurements correspond to excitations of much higher momenta than those active in the IR. Even aside from the quite probable wavelength dependence of damping, its effect on the frequency as q is varied changes quite markedly. For the larger q, one observes a line somewhat depressed in frequency and with a linewidth showing smaller apparent damping constant.

The neutron-scattering measurements in the cubic phase indicate, too, that the soft mode also appears lower in frequency and narrower in width than predicted by reflectivity data.[17] Also, the width measured (easily) for the LA_1 mode which, according to the reflectivity fits is part of the soft-mode system, is far too narrow to be in agreement with the large damping obtained in the said fits.

In summary, we have shown the presence in the Raman spectrum of tetragonal $BaTiO_3$ of a low-frequency mode with the right properties to be a good candidate for the softest ferroelectric vibration; we have also identified three pairs of L-T A_1 modes where frequencies semiquantitatively satisfy the LST relation; the soft-mode result has been discussed in terms of the effect of damping on the dispersion relation. Based on these measurements, it is possible to provide an almost complete assignment for the $\mathbf{q}=0$ optic modes in tetragonal $BaTiO_3$.

ACKNOWLEDGMENTS

We wish to acknowledge enlightening discussions with Dr. H. Stadler and Dr. T. Kushida, and the very expert technical assistance of R. Kilponen in the carrying out of these experiments.

[28] A. H. Meitzler and H. L. Stadler, Bell System Tech. J. **37**, 719 (1958).

[29] T. S. Benedict and T. L. Durand, Phys. Rev. **109**, 1091 (1958).